

# Nonlinear physical processes of accretion flows - results and developments

Krasimira Yankova, Lachezar Filipov, Daniela Boneva, Dejan Gotchev  
Space Research and Technology Institute, Bulgarian Academy of Sciences, BG-1113, Sofia  
f7@space.bas.bg, lf Filipov@space.bas.bg, danvasan@space.bas.bg,  
dejan@space.bas.bg

(Submitted on 16.11.2013. Accepted on 08.06.2014.)

**Abstract.** The theory of accretion and accretion discs takes a central place in the modern astrophysics. The main aim of our research is based on the exploration of the accretion flow dynamics through the application of theoretical and observational methods in compact objects. The applicability of hydrodynamical (HD) and magnetohydrodynamical (MHD) models and simulations on the study of accreting astrophysical objects evolution is analyzed. We develop numerical and analytical models to investigate the emergence of instability, wave propagation and structure formation in non-stationary accretion flows. A model able to provide the transition of 3-Dimensional turbulence to 2-Dimensional one is also proposed. The results show that during the evolution process, the accreting flow undergoes structural transformations and then they could be responsible for some known observational effects.

**Key words:** Accretion, accretion discs; Hydrodynamics; Magnetohydrodynamics; Waves; Methods: numerical; (Stars): binaries: close;

## Introduction

We present our recent results on the dynamics and structure of accreting flow in astrophysical matter. The research concerns the astrophysical objects, such as: Close Binary Stars (CBSs) with accretion discs and Active Galactic Nuclei (AGN). Around the massive black holes in these objects, there are discs that cannot be cooled efficiently, because the release of energy in them is much faster than the speed of its transformation into radiation. Flows in advective discs are non-stationary (Chen et al. 1997) by nature. The time of inflow is short and the dissipation works faster than the diffusion. The disc cannot emit all the released energy. Some of it is converted into heat and remains inside the disc.

Advection alters the balance in the disc (Beloborodov, 1999; Bisnovatyi-Kogan, 1998) and it leads to a new kind of a steady-state, but this steady-state is not an equilibrium. Advective accretion flows, in particular, are divided into two types (Beloborodov, 1999; Bisnovatyi-Kogan, 1998; Bisnovatyi-Kogan, 1999; Chen et al. 1997; Narayan et al., 1997; Narayan & Yi, 1995): optically thick and optically thin flows. The advection in the optically thick disc takes place with higher accretion values and smoothes out the thermal instability. The advective flow captures the radiation and brings it to the smaller radii along with the flow (Chen et al. 1997; Narayan & Yi, 1995). In an optically thin disc high-temperature maintains the ion-pressure high, and thus provides strong viscosity. Because of the low density, it is difficult to transmit the energy released to the electrons. Thus, the disc cannot be cooled effectively by the radiation. The main energy remains in the accretion flow and increases the effective temperature  $T_e$ , which could cause the advection to appear in these discs (Bisnovatyi-Kogan & Lovelace, 2002).

Vortices play a key role in the accretion disc dynamics, because they are considered as an efficient mechanism of angular momentum transportation

(Baranco & Marcus, 2005). At present, there are many hydrodynamics numerical studies dedicated to the way of appearance of vortices and their behavior in the flow. Shen et al. (2006) examine the formation of 2D vortices starting from 2D turbulence in fully compressible simulations. Baranco & Marcus (2005) compute the evolution of 3D vortices and show that part of the vortical formations could be destroyed, but the other part survive for several hundreds of orbits.

By performing a series of runs with zero initial vorticity and perturbation wavelengths, Johnson and Gammie (2006) give a very realistic way of the initial vorticity generation. They have noted that the remaining vorticity can be generated from "finite-amplitude compressive perturbations". They also give an interesting research in (Johnson & Gammie, 2005), where they argue that the vortices are "long-lived" assuming the formations could not be conserved in 3D calculations.

The results of our paper demonstrate how the patterns evolve in studying astrophysical discs. An effect of their local development in the inner disc's structure configuration is shown. The aim of our theoretical research is to track the evolution and to interpret the mechanisms of the high energy behavior of sources, such as: CBSs and AGN.

## 1. The background of the problem: Basis and methods.

### 1.1. Magnetohydrodynamical (MHD) approximation

The basic equations of magneto-hydrodynamics for non-stationary and non-axisymmetrical accretion flows are investigated. We have developed a new model of the accretion disc's magnetohydrodynamics, based on some specific advective hypothesis, presented in (Yankova, 2013) and described in the subsection below. We constructed geometrically thin, optically thick, one-temperature Keplerian disc in a normal magnetic field, around a black hole. The results of the model, given in detail in (Iankova, 2007; Iankova, 2009; Iankova & Filipov, 2010), allow us to: observe the evolution of the disc; investigate the emergence of the disc's instability; study the generation of its corona.

**Advective hypothesis.** Many authors, among them (Bisnovatyi-Kogan, 1998; Bisnovatyi-Kogan, 1999; Bisnovatyi-Kogan & Lovelace, 2002; Hawley & Balbus, 2002; Igumenshchev & Abramovich, 2000), have considered advective-dominated sub- and super-Eddington flows. The more popular models suggest a flow deformation, such as: 1) rotation of the velocity vector - in the form of a sharp increase in the radial velocity and a significant decrease of the orbital velocity to sub-Keplerian values; 2) orbital advection for low magnetic discs, where the maximum speed of sound is dominated by the Keplerian rotation (Fabian et al. 2012).

In our research, in contrast to these models, we provide the advection in the form of the complete advective term, which is naturally produced in the equations describing the flow dynamics. To explain our hypothesis, we transform the left part of the model equation of motion in a form derived from Iankova (Iankova, 2007). This yields the next expression:

$$\frac{\partial(\rho v_i)}{\partial t} + \frac{\partial}{\partial x_j}(\rho v_i v_j) = \rho \left( \frac{\partial v_i}{\partial t} + v_j \frac{\partial v_i}{\partial x_j} \right) = \rho \frac{Dv_i}{Dt} \quad (1)$$

Here  $v$  is the flux velocity;  $\rho$  - mass density;  $x_i$  is the spatial coordinate and operator  $\frac{D}{Dt}$  defines a complete advective term. So, the result of this transformation shows that there is not any increase of the radial velocity. In fact, the form of the complete advective term doesn't indicate the individual modification of one or the other of the velocity components. This means that a shifting arises of the average flow with velocity  $v_i$  in any direction.

In a case, when the advection is non-dominant mechanism, there isn't a condition for any flow deformations. The full advective term transfers the solution as a whole. In contrast to the other models, (although they can be considered as particular cases), no rotation or lengthening of the velocity vector appears here. The physical meaning of the vector's rotation in models with radial advection, see (Beloborodov, 1999; Bisnovaty-Kogan, 1998; Bisnovaty-Kogan, 1999; Chen et al., 1997; Narayan et al., 1997; Narayan & Yi, 1995), is that the action of  $\frac{\partial v_i}{\partial t}$  is ignored. An orbital advection, by (Fabian et al. 2012), is a superposition of an orbital speed vector that is added to the Keplerian velocity. At this type of advection, the nature of the process requires the linearization in the model equations.

In the powerful gravitational field of the black holes, the advection of a "complete term" type (see the equation above) has the highest rate of probability to arise. During the disc's development in a normal dipole field, the term  $B_r B_\varphi$  of the equation of motion creates the conditions for the radial advection (Campbell et al. 1998) in the flow. Thereby, we can unambiguously determine the direction of the disc's middle flow displacement. A radial pulling into a black hole with complete advection can lead the inflow speed to about the half of the free fall rate, without any weakening of the orbital rotation. In fact, exactly the opposite is true, when the redistribution of the momentum in a dipole field is accelerating the rotation. Then, the viscous and dynamic time-scales are comparable and they are shorter than the thermal scale. This way, the cooling process becomes inefficient. The above described conditions give rise to the self-induced advection activity.

As it brings the flow to the new orbit, the advection can only indirectly control the velocity components. The orbital velocity is Keplerian again, because the flow does not change its nature in the case of such a packet transfer. The changes in the orbital rate reflect to the other velocity components coherently, because of the "complete term" type of advection.

The advection in similar conditions can work for relatively lower temperatures in the outer regions of the disc. The earlier advection appearances guarantee that the flow will remain optically thick at the temperatures of first and second orders, which is higher than the normally accepted one. In the heat balance equation, the advection works in the same way - it extracts the heat to the disc's centre and provides the energetic structural formation at small radii. The main results of the model are shown in (Iankova, 2007; Iankova, 2009; Iankova & Filipov, 2010; Yankova, 2013).

## 1.2. Hydrodynamical (HD) approximation

The essence of physical processes in the interacting flows allows employment of gas-dynamics equations. We apply the basic equations in a form that have been suggested and affirmed by many authors: (Clark & Carswell, 2007; Frank et al., 2002; Graham, 2001; Shu, 1992). We have modified the parameters partially and thereafter the equations are presented in their applicable form in (Boneva & Filipov, 2012). They are as follows: equation of mass conservation, Navier-Stokes equations, energy balance equation, equation of state for compressible flow and vortical transport equation. We employ the vortical transport equation, because of its relation to the examination of transfer's mechanisms in the flow. This equation could be derived in the following commonly used way, as it has been done by Nauta (2000), Lithwick (2007), Godon (1997). The idea was initially proposed by (Klahr & Bodenheimer, 2003). If the curl of Navier-Stokes equations is considered, and the next expressions are used:  $\Psi = \nabla \times v$  - expressing the vorticity in the flow;  $(v \cdot \nabla) v = \nabla \frac{v^2}{2} - (v \times \Psi)$  and  $\left( \frac{\partial \Psi}{\partial t} + v \cdot \nabla \right) \frac{1}{\rho} = \frac{\nabla \rho \times \nabla P}{\rho^3}$ ; then the following expression is obtained:

$$\frac{\partial \Psi}{\partial t} + \Psi (\nabla \cdot v) + (v \cdot \nabla) \Psi = - \frac{\nabla p \times \nabla \rho}{\rho^2} + D \nabla^2 \Psi \quad (2)$$

Here  $\Psi$  is the vorticity;  $D$  is the diffusion coefficient (or matrix of the transport coefficient).

This equation expresses the relation between the transport coefficient, which takes part in the angular momentum transfer, evolution of the vorticity with time and the non-conserve relationship between density and pressure in the flow. Non-conservancy of specific vorticity by each fluid element is observed in the right-hand side of the equation.

On the base of numerical codes, the model of box-framed scheme has been suggested and applied. This way, we could perform the calculations in limited regions of all disc's areas by configuring the scheme for each problem. Then, we make the calculations inside the box, or frame with different measurement. The used methods are implicated into the codes and these are: the Runge-Kutta (implicit part) method - treats every step in a sequence of steps in identical manner. That fact makes it easy to add in Runge-Kutta into relatively simple schemes; Alternating direction implicit method (ADI) - based on finite difference scheme and following the idea to split the finite difference equations in two. They are implicit methods, which are general in their application. It is suitable to use them in the solutions of partial differential equations, because of their high stability.

## 2. Results

In the MHD analysis, on the base of the new hypothesis, explained in Section 1.1. and (Yankova, 2013), we introduced a modification function

$$F_i = F_{i0} \Re_i \left( x = \frac{r}{r_0} \right) \exp [k_\varphi(x) \varphi + \omega(x) t] = F_{i0} f_i(x) \quad (3)$$

for leading parameters in the model's equations (Iankova, 2007). We obtain global solutions for the 2D and 3D structures and local evolution of accretion disc.

The results are presented in cylindrical coordinates. Dimensionless distributions of the main physical features  $f_i(x, \varphi)$  describe the decisions for radial and local structures of the disc in equatorial plane  $(X, Y)$ . Where

$$(X = x \cos \varphi, Y = x \sin \varphi), \quad x \in (x_g, 1) \quad \left(x_g = \frac{r_g}{r_{out}}\right)$$

in the radial structure and  $x$  is measured in  $r_g$  units for the local structure.

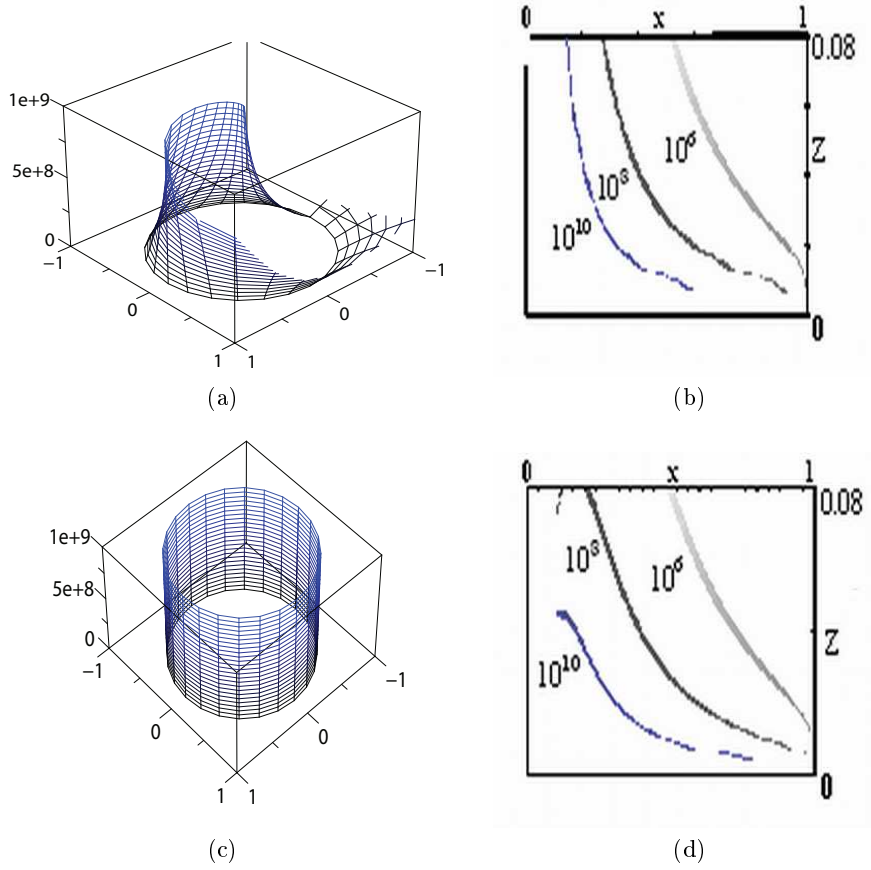


Fig. 1: The distribution of dimensionless function of the equatorial density  $f_1(X, Y)$  in non-axisymmetric MHD model, presented in a 3D boxed scheme  $[-1, 1]$  (Fig.1(a), 1(c)). Figures 1(b), 1(d) show the profiles  $(x, Z)$  in 3D, for densities contours  $f_1(x, Z) = 10^6; 10^8; 10^{10}$  at the moments  $t = 1P$  and  $t \sim 0$

A synchronic interpretation of both the radial and the local distributions of the disc's physical parameters indicates the presence of a specific type of structures that are formed during the evolution. The presence of helix' mega-structures can be registered by the result of mass density (Figs. in Iankova,

2007; Iankova, 2009). Fig.1a shows a surface distribution of the equatorial density. The split in the surface of the function shows an existence of one spiral. In the simulations of the Bisikalo's group, it has shown that at the temperatures higher than  $10^6$  the hot discs have only one tidal spiral. Further, at a moment  $t \approx 0$  (Fig.1b), the matter is accumulated mainly into the ring at the orbit  $x \approx 0.8$  and is slowly spreading inside. This spreading can be seen in the profiles for the key moments  $t = 1P$  and  $t \approx 0$ , as well.

The results of 2D disc's structure show the appearance of short-live ring-formations, with an enhanced density (Iankova & Filipov, 2010). We build a model of such a formation and we obtain an expression for the local heating and local developments of the flow's characteristics. The behavior of the averaged local heating, which is built by the local model:  $K(x) = \frac{\text{warming}}{\text{cooling}}$  and the global development of the entropy gradient  $\partial_t s$  shows that the internal disc's structure gradually alters into a new dynamic state - relatively stable, but very far from equilibrium.

We can register a vortex in a 2-dimensional structure. It could be clearly seen both in the radial velocity's local behavior and in the magnetic field.

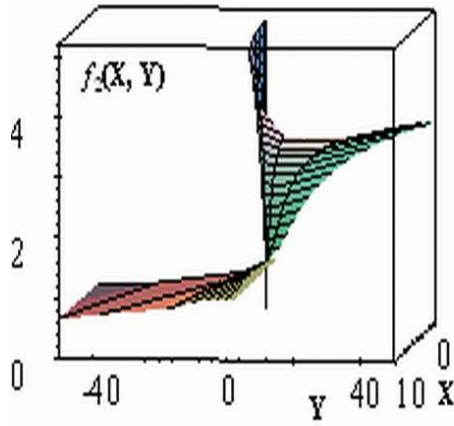


Fig. 2: Local development of the dimensionless radial velocity  $f_2(X, Y)$  shows two individual branches of the function, with properties in morphology - the top branch is folded additionally. A different grid scale is used in the calculations for this model.

In Figure 2, the upper branch shows that the inflow is additionally folded. In these places, the radial velocity rapidly decreases, and then its rotating component is the only important. Figure 3 shows a presence of rotation in the magnetic field's radial component. The velocity function is folded in the same area where the field is rotated and a vortex-microstructure is localized there (Fig. 2, 3).

In the next calculations by the HD approximation, we can see that the changes in the mass transfer rate are in a close relation both with disturbances in the density and in the velocity. On the base of the perturbation analysis in hydrodynamical flows, we have studied in detail variations of the flow param-

eters, in (Boneva & Filipov, 2012; Boneva, 2009). To study this, we apply the modified perturbation function, described in (Boneva, 2009), on the Navier-Stokes equations. The perturbations are chosen to be in an exponent form with a power of second order and the velocity perturbations have the form:  $u(r, \varphi) \approx u \exp(im^2\varphi - i\omega t)$ . This form is applied also to the other quantities. Here  $\omega$  is the wave number and  $m$  is the mode number of  $\varphi$  direction. Let us first write down the already introduced in (Boneva, 2009) perturbation quantities into the flow parameters:  $V = v + u$ ;  $\rho_0 = \rho + \rho'$ ;  $p = P + p'$ . where  $V, \rho_0, p$  are the total quantities of velocity, density and pressure, respectively;  $v, \rho, P$  are the time averaged values;  $u, \rho', p'$  are the perturbations in time. Next, we apply them into the Navier-Stokes equations. The behavior of perturbed velocity is calculated for different values of the dimensionless parameter  $m$ . We use a grid-scale measurement of values  $[30, 30, 30]$ , which is more suitable to detect the results. The next initial values are applied:  $V(0) = V_0$ ,  $u(t_0) = u_0$ ,  $t_0 \approx 1$ ,  $r_0 \approx 1$ . It results in occurrence of velocity excess during the period of disturbance (see Fig. 4). After the calculations, we detected sharp decrease of velocity values. The sequence of the full process was shown in (Boneva & Filipov, 2012, see Appendix) and (Boneva, 2009). Here we receive a "collective" result and we can see the total quantity of the velocity  $V = V_t$ .

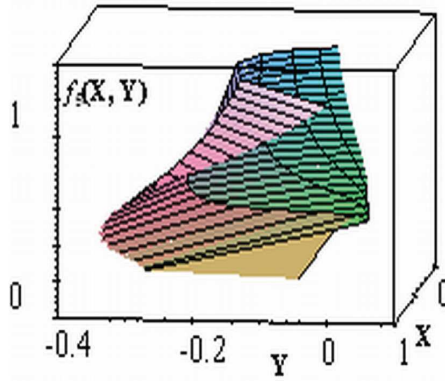


Fig. 3: Local development of the radial component of the magnetic field shows almost complete rotation of the vector.

The velocity behavior could be related to some local unstable activity in the accretion discs zone (e.g. the change of mass transfer rate of the inflow matter in close binary). The scales of the axes are constrained by the parametrization of the code.

In the places where the velocity values are close to their minimum, the density starts to increase and it pulls matter there. Thereafter, this means that the matter from a disc could be pumped out or concentrated within given places, causing the density's dilution in close areas. In the paper (Boneva & Filipov, 2012), we have obtained the results that show the appearance of area with increased density, the "thickened zone". The calculations were performed for 4.5 orbital periods of rotation. The graphical results there depict four time

stop-steps for one rotational period only. In accordance to the "thickened zone" formation and in a relation to the variability in density, we obtain the solution for density values in these places.

The variability in density, in accordance to the "thickened zone" formation, gives an information about the matter accumulation in the defined area by the boundary conditions. Graphical view of the high density value places is in a pillar-like form. The composite result (see Fig.5) points that four time steps again for one rotational period and corresponds to the figure of "thickened zone" in papers (Boneva & Filipov, 2012 - see fig. 1; Boneva et al, 2013).

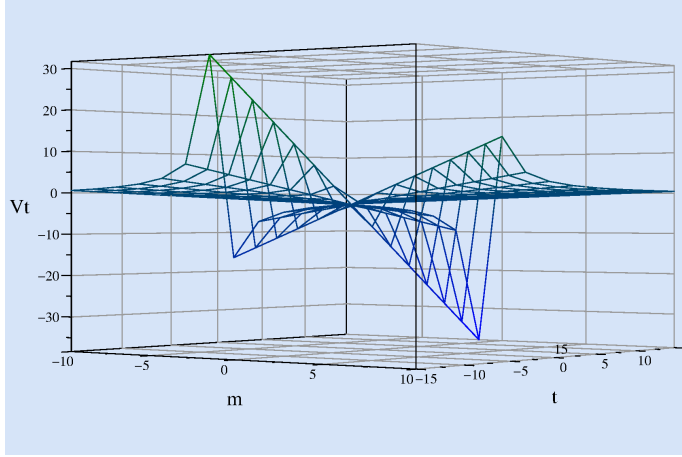


Fig. 4: Velocity variations in the flow during the mass transfer. The process for different values of  $m$  is seen. Variations start at  $-0.45 > m \leq -1$ . When the values of  $m$  start to decrease ( $m \leq -1$ ) the process reverses. The critical value is at  $m = -3$ . This leads to a fission in the solution and a suddenly drop off in the velocity values is observed.

The results show that during the 4.5 orbital periods of rotation, the dense areas keep its shape and size. It can be concluded that the thickened zone could exists for a long period of time and it does not change its mean characteristics over the time of our calculations.

As in the paper (Boneva et al. 2013), we confirm here our comparison of the 2-dimensional vs. 3-dimensional single vortex formation. First we point to the 2D simulation made by (Boneva & Filipov, 2012; Boneva, 2010). Fig.6a presents a single vortex formation, which is a part of pattern configuration frame in the covered range of about  $7.687 \times 10^{-8}$  AU to  $6.68 \times 10^{-7}$  AU.  $K(x, y)$  is the boundary calculation area.

A computational analysis is performed to reveal one possible way of their appearance by visual simulation of their development in the flow. Our calculations are based on the vortical transport equation in the form obtained in (Boneva & Filipov, 2012), see Section 1.2. The box-frame model is used once again. The picture (Fig.6a) visualizes the final stage of vortex-like development in the flow. For this final run of calculations the density and velocity accepted



values  $\rho(t_n), v(t_n)$  are used as an input. Then, we consider the stage of vortex evolution in some steady period of their development, when they are "ready" for the angular momentum transport.

The light blue and dark blue colors show the difference in density in the interacting flow layers. The density values are increasing from the light to the dark zone. According to the conditions of the general flow and by applying the simulations again, we obtain the 3D view of the single vortex evolution in the accreting flow. The box boundary values in this case are:  $K(x, z, y) \in 8 \times 10^{-9} AU$  to  $7 \times 10^{-10} AU$ . The 3-dimensional vortex-like formation is presented as a patch graphics in the calculating mesh grid in Figure 6b. Unlike the 2-dimensional calculations, here we perform the runs with non-zero initial vorticity and non-zero initial turbulization. In this paper, we chose to employ the single vortex configuration in order to look at the formation in detail. This way we can make a better comparison between the 2D and 3D development. Then, an initial deformation in the single vortex-like 3-D configuration is observed. Our three-dimensional results are still under investigation and the problem will be solved in the near future.

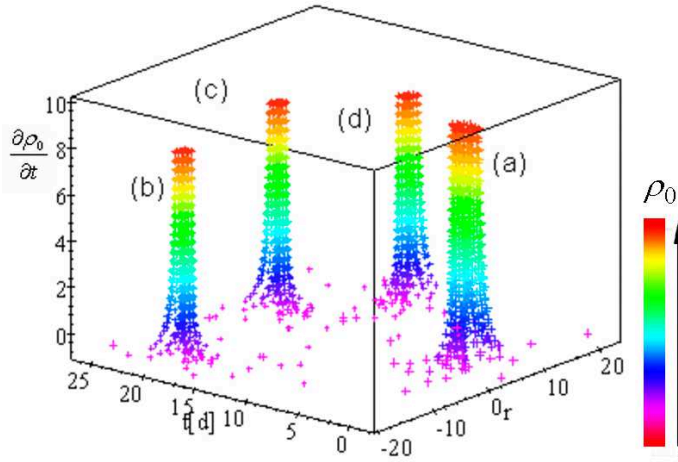


Fig. 5: Pillar's form graphical expression of density concentration in close area. The image shows the accumulating matter in four moments of time in a rotational period. Calculations are made in 3D quadratic frame in  $x, y$  and on variations of the perturbed density value  $\rho'$ .

We analyze our results on the MHD model for key moments  $t = 1P$  and  $t \sim 0$  in the next steps: Consideration of the radial and vertical structure of the disc; Development of the stratification condition  $|v_a| \leq |v_s|$ ; Coset with the vector field of the velocity  $(v_r, v_z)$ ; Comparison of the coefficients of the meeting of the global model with wave numbers in the local model. We can conclude that the disc develops a spherical radiative (non-convective) corona (Iankova & Filipov, 2010; Yankova, 2013). The disc model is modified according to the conditions of the disc's corona. The future aim is to make possible

piecing together the both solutions, in a case when the two global flows have no common energetics.

## Conclusion

A similar flow's nature is observed in the results received independently from both HD and MHD approximations. There appeared zones with increased density in some places of the accretion flow. The shapes and sizes of these zones are different in advective and nonadvective disc. This could be caused by the influence of the difference in their temperature values over the other disc's parameters. In both cases a development of vortical structures is detected on the boundaries of the thickened and diluted area. The vortexes are obtained both in our analytical considerations and in the numerical calculations.

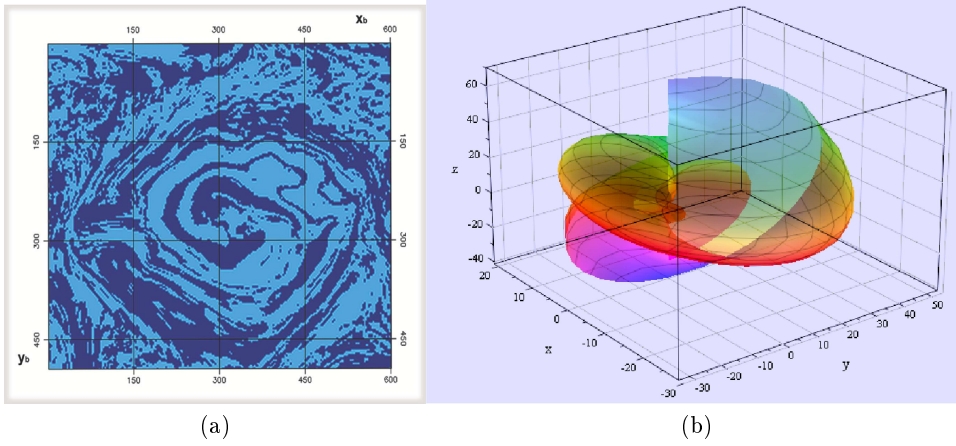


Fig. 6: Single vortex like pattern as a result of 2D calculations, with zero initial vorticity, but with initial present turbulization value different from zero. The boundary calculation area  $K(x, y)$  covers of about  $7.687 \times 10^{-8} \text{AU}$  to  $6.68 \times 10^{-7} \text{AU}$ , Fig.6a. 3D result of a single vortex-like structure, with non-zero initial vorticity and function of turbulization. The boundary calculation area  $K(x, z, y)$  covers of about  $7.687 \times 10^{-9} \text{AU}$  to  $6.68 \times 10^{-10} \text{AU}$ . The picture shows decomposition in the vortex formation stage, Fig.6b

We come to the next conclusions: The employment of two independent methods of approach in the same area of research gives similar results. This way, the validity of the created models is confirmed. Our theoretical study allows to make a qualitative analysis of the physical processes in real astrophysical objects of research. Therefore, it could be applied for the future investigations of the accretion disc's acting mechanisms, that are still not yet well understood.

## References

- Barranco J. A., Marcus P. S., 2005, *ApJ*, 623, 1157
- Beloborodov A. M., 1999, *ASP Conf. Ser.*, 161, 295
- Bisnovatyi-Kogan G.S., 1998, *Observational Evidence for the Black Holes in the Universe, Conference held in Calcutta*, 1, arXiv: astro-ph/9810112
- Bisnovatyi-Kogan, G.S., 1999, *Odessa Astronomical Publications*, 12, 169, arXiv: astro-ph/9911212
- Bisnovatyi-Kogan, G.S., Lovelace, R.V.E., 2002, *New Astron. Rev.*, 45, 663
- Boneva D.V., 2009, *BgAJ*, 11, 53
- Boneva D.V., 2010, *BgAJ*, 13, 3
- Boneva D., Filipov L., 2012, Density distribution configuration and development of vortical patterns in accreting close binary star system, <http://adsabs.harvard.edu/abs/2012arXiv1210.2767B>
- Boneva D., Filipov L., Gotchev D., 2013, *Publ. Astron. Soc. Rudjer Boskovic*, 12, 113–114, <http://wfpdb.org/ftp/8SBACD1/pdfs/07.pdf>
- Campbell C. G., Papaloizou J. C. B., Agapitiu V., 1998, *MNRAS*, 300, 315
- Clark C., Carswell R., 2007, *Principles in Astrophysical Fluid Dynamics*, Cambridge University Press
- Chen X., Abramowicz M. A., Lasota J.P. 1997, *ApJ*, 476, 61
- Fabian A.C., Wilkins D.R., Miller J.M., Reis R.C., Reynolds C.S., Cackett E.M., Nowak M.A., Pooley G.G., Pottschmidt K., Sanders J.S., Ross R.R., Wilms J., 2012, *MNRAS*, 2012, 424, 217
- Frank J., King A., Raine D., 2002, *Accretion Power in Astrophysics*, 3rd edition, Cambridge University Press, New York
- Graham J.R., 2001, *Astronomy 202, Astrophysical Gas Dynamics*, Astronomy Department, UC Berkeley
- Godon, P., 1997, *ApJ*, 480, 329
- Hawley J.F., Balbus S.A., 2002, *ApJ*, 573, 749.
- Iankova Kr.D., 2007, Accretion disc with advection and magnetic field, *Conf. Ser. Black Sea School on Plasma Physics*, <http://sp.phys.uni-sofia.bg/Kiten06/Pres/Iankova.pdf>
- Iankova Kr.D., Filipov L., 2010, Structure of a magnetized accretion disc, *Proceedings of SENS 2009*, 370, BULGARIA, <http://www.space.bas.bg/SENS2009/7-A.pdf>, ISSN 1313 3888
- Iankova Kr.D., 2009, Stability and evolution of magnetic accretion disc, *Publ. Astr. Soc. Rudjer Boskovic*, 9, 327, <http://aquila.skyarchive.org/6SBAC/pdfs/31.pdf>
- Igumenshchev I.V., Abramovich M.A., 2000, *ApJ*, 130, 463
- Johnson B. M., Gammie C. F., 2005, *ApJ*, 635, 149
- Lithwick, Y., 2007, *ApJ*, 670, 789L
- Narayan R., Kato S., Honn F., 1997, *AJ*, 476, 49
- Narayan R., Yi, 1995, *ApJ*, 452, 71
- Nauta, D., 2000, Two-dimensional vortices and accretion disks, *University Utrecht press*
- Shu F.H., 1992, *The Physics of Astrophysics*, Vol 2, Gas Dynamics, University Science Books.
- Yankova K., 2013, Generation and development of the disc corona, *Proceedings of 8th SBAC, Publ. Astron. Soc. Rudjer Boskovic*, 12, 375, <http://wfpdb.org/ftp/8SBACD1/pdfs/34.pdf>